GEOPHYSICS, VOL. 68, NO. 6 (NOVEMBER-DECEMBER 2003); P. 1817–1821, 3 FIGS.
10.1190/1.1635034

Short Note

Effective anisotropy of layered media

Andrey Bakulin* and Vladimir Grechka*

INTRODUCTION

In-situ seismic anisotropy can be estimated using a variety of techniques. Since they require data that are typically collected over some finite intervals of inevitably heterogeneous earth, one usually needs to separate the influence of anisotropy on the measurements from that of heterogeneity. It is not an easy task because, depending on the frequency of propagating waves, heterogeneity and anisotropy might mimic each other. The well-known example of this is a finely layered isotropic solid that effectively behaves as a vertically transversely isotropic (VTI) rock when probed by sufficiently long seismic waves (Backus, 1962). Similar transitions from heterogeneity to anisotropy and back occur over the whole range of seismic frequencies. For instance, Grechka and Tsvankin (2002) recently showed that a layered isotropic structure also looks like a VTI one at high frequencies, when the ray tracing and Dix-type averaging of the normal moveout (NMO) velocities can be applied.

In our view, part of the difficulty in discriminating the influences of intrinsic anisotropy and heterogeneity on seismic data stems from the inherent complexity of wave propagation in heterogeneous anisotropic media. Even restricting the models to 1D horizontally layered media does not fully eliminate the problem. Indeed, the effective stiffnesses $\mathbf{c}^e$ in the low-frequency regime are computed by performing Schoenberg-Muir calculus (Schoenberg and Muir, 1989) that operates with elements of the interval stiffness tensors $\mathbf{c}$ arranged in 3×3 matrices. At high frequencies, when the effective NMO velocities are relevant for describing seismic data, the anisotropic counterpart of the conventional Dix (1955) formula averages the NMO ellipses represented by 2×2 matrices $\mathbf{W}$ (Grechka et al., 1999). Given such a complexity (which increases at intermediate frequencies due to scattering) and the usual inaccuracies in the estimated anisotropy that preclude a geophysicist from choosing the best possible model, it is not surprising that physical intuition regarding the interplay between anisotropy and heterogeneity has not yet been developed.

The goal of our short note is to show that this interdependence is often not strong and, therefore, can be ignored. Specifically, we will demonstrate that all averaging techniques are equivalent up to the quadratic terms in fluctuations $\tilde{\mathbf{m}}$ of layer velocities, densities, and anisotropies from their mean (i.e., volume average) values $\bar{\mathbf{m}}$. As a consequence, the errors made by replacing the properly computed effective anisotropic coefficients $\boldsymbol{\Delta}^e$ with their means $\bar{\boldsymbol{\Delta}}$ are expected to be small under the assumptions of weak anisotropy and small velocity and density contrasts at layer interfaces. Bakulin (2003) drew this conclusion for two-component finely layered VTI media. Here, we show that it remains valid for much broader range of anisotropic models and seismic frequencies. The generality of our results suggests that many available measurements of in-situ anisotropy are probably relatively weakly contaminated by unaccounted heterogeneity (unless it is uncommonly strong) and, therefore, tend to indicate the presence of intrinsic anisotropy which may be related to the properties of rock fabrics, fractures, or in-situ stresses. On the other hand, a pure heterogeneity-induced anisotropy, such as that produced by Backus averaging of isotropic finely layered media, is usually weak because it is quadratic in terms of relative changes in the velocities and density.

We begin with examining the general procedure used to compute parameters $\mathbf{m}^e$ of effective media and, then, prove our main statement that the differences in effective and average quantities occur in the second- and higher-order terms in fluctuations $\tilde{\mathbf{m}}$. Next, we verify our theoretical conclusions numerically using a typical well log with intentionally added moderate anisotropy. Throughout the paper, we denote the interval (local) quantities and their corresponding volume averages, fluctuations, and effective quantities as $\mathbf{m}$, $\bar{\mathbf{m}}$, $\tilde{\mathbf{m}}$, and $\mathbf{m}^e$, respectively.

LOCAL AND EFFECTIVE QUANTITIES

In this section, we discuss the general relationship between a pair of interval and effective quantities, $\mathbf{m}$ and $\mathbf{m}^e$. Quite

Manuscript received by the Editor December 3, 2002; revised manuscript received June 3, 2003.
*Shell International Exploration and Production, 3737 Bellaire Blvd., Houston, TX 77025. E-mail: andrey.bakulin@shell.com; vladimir.grechka@shell.com.

remarkably, all known averaging procedures applied to either tensors, or matrices, or scalars $\mathbf{m}$ and $\mathbf{m}^e$ can be represented in the form

$$\mathbf{F}[\mathbf{m}^e] = \frac{1}{V}\int_V \mathbf{F}[\mathbf{m}(\mathbf{x})]d\mathbf{x}, \tag{1}$$

where $\mathbf{F}$ is the operation that averages the quantity $\mathbf{m}(\mathbf{x})$ over the representative volume V (which can be also an area or a linear segment), and $\mathbf{x} \equiv [x_1, x_2, x_3]$ denotes Cartesian coordinates.

Although the functions $\mathbf{F}$ are different for different averaging procedures (see the examples below), they share two important properties: differentiability and invertibility. The first property means the existence of derivatives $D\mathbf{F}/D\mathbf{m} \equiv \partial F_i/\partial m_j$, where F_i and m_j denote the elements of tensors $\mathbf{F}$ and $\mathbf{m}$. The invertibility states that there is such a function $\mathbf{F}^\dagger$ which undoes $\mathbf{F}$, i.e.,

$$\mathbf{F}^\dagger[\mathbf{F}[\mathbf{m}]] = \mathbf{m} \quad \text{and} \quad \mathbf{F}^\dagger[\mathbf{F}[\mathbf{m}^e]] = \mathbf{m}^e. \tag{2}$$

The latter allows us to rewrite equation (1) as

$$\mathbf{m}^e = \mathbf{F}^\dagger\left[\frac{1}{V}\int_V \mathbf{F}[\mathbf{m}(\mathbf{x})]d\mathbf{x}\right]. \tag{3}$$

Examples of functions F

Since any averaging procedure can be cast in the form of equations (1) or (3), the examples of functions $\mathbf{F}$ are abundant. Perhaps, the simplest one is the Backus (1962) average of Lamè constants μ in a stack of plane thin isotropic layers that yields the stiffness coefficient c_{66}^e of the effective VTI medium:

$$c_{66}^e = \frac{1}{V}\int_V \mu(\mathbf{x})d\mathbf{x}. \tag{4}$$

Clearly, equation (4) is a special case of equation (1) when both $\mathbf{F}$ and $\mathbf{F}^\dagger$ are the scalar identity functions whose values are equal to those of their arguments, $F[m] = F^\dagger[m] = m$.

Another well known example is the Backus average of μ that produces the effective stiffness c_{44}^e:

$$c_{44}^e = \left[\frac{1}{V}\int_V [\mu(\mathbf{x})]^{-1}d\mathbf{x}\right]^{-1}. \tag{5}$$

This time, equation (5) follows from equation (3) if we let functions $\mathbf{F}$ and $\mathbf{F}^\dagger$ be the inverse of their scalar arguments, i.e., $F[m] = F^\dagger[m] = m^{-1}$.

A more complicated Schoenberg-Muir calculus, which extends Backus averaging to anisotropic media, can be also written in the form (3). Instead of showing this directly, we refer the reader to Appendix A, where we prove a much more general statement valid in 3D heterogeneous anisotropic media.

Other averaging procedures, for instance, the Dix (1955) formula for the NMO velocities v,

$$v^e = \left[\frac{1}{T}\int_0^T v^2(t)dt\right]^{1/2}, \tag{6}$$

where T is the vertical time, and the generalized Dix formula of Grechka et al. (1999) for the NMO ellipses (2×2 matrices) $\mathbf{W}$,

$$\mathbf{W}^e = \left[\frac{1}{T}\int_0^T \mathbf{W}^{-1}(t)dt\right]^{-1}, \tag{7}$$

can be also reduced to equations (1) or (3) that perform spatial rather than temporal integration. The way to show this is to change the differential dt in equations (6) and (7) to $q dx_3$, where q is the vertical slowness and x_3 is the depth. We skip these proofs because they exactly repeat the one described in Appendix A.

PROOF OF RELATIONSHIP $\mathbf{m}^e = \bar{\mathbf{m}} + O(\tilde{\mathbf{m}}^2)$

Having presented a number of examples showing the validity of equations (1) and (3), we are ready to formulate our main statement. First, however, we need to define the mean $\bar{\mathbf{m}}$ and fluctuation $\tilde{\mathbf{m}}(\mathbf{x})$ of $\mathbf{m}(\mathbf{x})$:

$$\bar{\mathbf{m}} = \frac{1}{V}\int_V \mathbf{m}(\mathbf{x})d\mathbf{x} \tag{8}$$

and

$$\tilde{\mathbf{m}}(\mathbf{x}) = \mathbf{m}(\mathbf{x}) - \bar{\mathbf{m}}. \tag{9}$$

Note that the mean $\bar{\mathbf{m}}$ is calculated over the same representative volume V. As follows from equations (8) and (9),

$$\int_V \tilde{\mathbf{m}}(\mathbf{x})d\mathbf{x} = 0. \tag{10}$$

The equality we intend to prove reads

$$\mathbf{m}^e = \bar{\mathbf{m}} + O(\tilde{\mathbf{m}}^2). \tag{11}$$

Let us note the remarkable fact that $\mathbf{m}^e$ given by equation (11) does not contain any linear terms in fluctuation $\tilde{\mathbf{m}}$. To show this, we expand $\mathbf{F}(\mathbf{m})$ in a Taylor series in the vicinity of $\bar{\mathbf{m}}$,

$$\mathbf{F}[\mathbf{m}] = \mathbf{F}[\bar{\mathbf{m}}] + \left.\frac{D\mathbf{F}}{D\mathbf{m}}\right|_{\mathbf{m}=\bar{\mathbf{m}}} \tilde{\mathbf{m}} + O(\tilde{\mathbf{m}}^2), \tag{12}$$

and substitute this expansion into equation (3). We obtain

$$\begin{aligned}
\mathbf{m}^e &= \mathbf{F}^\dagger\left[\frac{1}{V}\int_V \left\{\mathbf{F}[\bar{\mathbf{m}}] + \left.\frac{D\mathbf{F}}{D\mathbf{m}}\right|_{\mathbf{m}=\bar{\mathbf{m}}} \tilde{\mathbf{m}}(\mathbf{x}) + O(\tilde{\mathbf{m}}^2(\mathbf{x}))\right\} d\mathbf{x}\right] \\
&= \mathbf{F}^\dagger\left[\mathbf{F}[\bar{\mathbf{m}}] + \frac{1}{V}\left.\frac{D\mathbf{F}}{D\mathbf{m}}\right|_{\mathbf{m}=\bar{\mathbf{m}}} \int_V \tilde{\mathbf{m}}(\mathbf{x})d\mathbf{x} + O(\tilde{\mathbf{m}}^2)\right] \\
&\qquad \text{because } \frac{1}{V}\int_V O(\tilde{\mathbf{m}}^2(\mathbf{x}))d\mathbf{x} = O(\tilde{\mathbf{m}}^2(\mathbf{x})) \\
&= \mathbf{F}^\dagger[\mathbf{F}[\bar{\mathbf{m}}] + O(\tilde{\mathbf{m}}^2)] \\
&\qquad \text{because } \int_V \tilde{\mathbf{m}}(\mathbf{x})d\mathbf{x} = 0 \text{ due to equation (10).}
\end{aligned} \tag{13}$$

Expanding function $\mathbf{F}^\dagger$ further in a Taylor series and making use of equation (2) yields

$$\begin{aligned}
\mathbf{m}^e &= \mathbf{F}^\dagger[\mathbf{F}[\bar{\mathbf{m}}]] + \left.\frac{D\mathbf{F}^\dagger}{D\{\mathbf{F}[\bar{\mathbf{m}}] + O(\tilde{\mathbf{m}}^2)\}}\right|_{\tilde{\mathbf{m}}=0} O(\tilde{\mathbf{m}}^2) + O(\tilde{\mathbf{m}}^4) \\
&= \bar{\mathbf{m}} + O(\tilde{\mathbf{m}}^2)
\end{aligned} \tag{14}$$

and, thus, proves equality (11).

It is critical to realize that since no formal relationship between the norms $\|\bar{\mathbf{m}}\|$ and $\|\tilde{\mathbf{m}}\|$ was used to establish equation (11), its value is not obvious because, in principle, relative magnitudes of the terms $\bar{\mathbf{m}}$ and $O(\tilde{\mathbf{m}}^2)$ can be arbitrary. On the other hand, the usefulness of equation (11) becomes clear when

$$\|\bar{\mathbf{m}}\| \gg \|\tilde{\mathbf{m}}\|. \tag{15}$$

Then, not only does equation (11) show that any effective quantity $\mathbf{m}^e$ is approximately equal to the mean value $\bar{\mathbf{m}}$ of the corresponding interval quantity $\mathbf{m}$, but it also states that the error one makes by replacing $\mathbf{m}^e$ with $\bar{\mathbf{m}}$ is expected to be small because it is quadratic with respect to the fluctuation $\tilde{\mathbf{m}}$. As a result, the approximation

$$\mathbf{m}^e \approx \bar{\mathbf{m}} \tag{16}$$

might be acceptable in many practical applications.

NUMERICAL EXAMPLE

Here, we demonstrate that approximation (16) works surprisingly well for typical layered media characterized by moderate polar and azimuthal anisotropy. We compare the performance of our approximation in predicting both the effective anisotropic coefficients $\mathbf{c}^e$ computed by Schoenberg-Muir calculus and the effective NMO ellipses $\mathbf{W}^e$ obtained using the generalized Dix formula (Grechka et al., 1999).

Figure 1 displays portions of typical Gulf of Mexico sonic, shear, and density logs measured over a 500-m interval with the increment 0.5 ft = 0.1524 m. Note that vertical velocity heterogeneity is not that weak. Its values, expressed through the differences between velocity maxima and minima divided by the mean velocities, are 49% and 51% for P- and S-waves, respectively. As we will see below, such velocity fluctuations do not cause our approximation to break down because the volumes occupied by extreme low- and high-velocity layers are relatively small. Next, we make all layers anisotropic, artificially introducing moderate monoclinic anisotropy specified by the coefficients $\boldsymbol{\Delta} \equiv \{\epsilon^{(1)}, \epsilon^{(2)}, \delta^{(1)}, \delta^{(2)}, \delta^{(3)}, \gamma^{(1)}, \gamma^{(2)}, \zeta^{(1)}, \zeta^{(2)}, \zeta^{(3)}\}$ (Grechka et al., 2000), whose values are Gaussian random numbers. The means $\bar{\boldsymbol{\Delta}}$ of these anisotropic coefficients in the whole model are shown with crosses in Figure 2.

To produce a suite of 300 anisotropic models, we keep the velocities and densities shown in Figure 1 fixed and randomly vary anisotropic coefficients in all layers. The standard deviations are equal to 0.10 for the interval $\epsilon^{(1,2)}$, $\delta^{(1,2,3)}$, and $\gamma^{(1,2)}$, and to 0.03 for $\zeta^{(1,2,3)}$. Given such large standard deviations, the local anisotropic coefficients $\epsilon^{(1,2)}$, $\delta^{(1,2,3)}$, and $\gamma^{(1,2)}$ would cover the whole range in Figure 2 if we plotted their interval values.

Assuming sufficiently low frequencies of propagating waves, we compute the exact effective medium for each of our 300 random models using Schoenberg-Muir calculus. The bars in Figure 2 indicate the ranges of effective anisotropic coefficients $\boldsymbol{\Delta}^e$. Quite remarkably, their values are well predicted by the means of the corresponding interval coefficients (crosses). This suggests a simple practical recipe for obtaining any given effective anisotropic coefficient Δ_i^e. Instead of going through Schoenberg-Muir computations in their full complexity, which would require knowing all interval velocities and anisotropies, one can just calculate the mean $\bar{\Delta}_i$ and use it as a reasonable estimate of Δ_i^e. Moreover, validity of this conclusion does not seem to depend on details of local parameter fluctuations. For example, the ranges of effective anisotropic coefficients shown in Figure 2 remain almost unchanged if Gaussian distribution of interval anisotropy is replaced with either uniform or log-normal distributions.

Figure 2 also demonstrates that some of the obtained means (e.g., $\bar{\delta}^{(1,2)}$ and $\bar{\gamma}^{(1,2)}$) are biased. The origin of these biases can be explained based on the Backus average of the original isotropic layered model (Figure 1) that produces a VTI solid with negative Thomsen (1986) anisotropic coefficient δ^e and positive γ^e. In accordance with our theory, such heterogeneity-induced effective anisotropy is weak, and the observed biases are much smaller than usual errors expected in anisotropic coefficients estimated from seismic data.

The effective normal-moveout velocities of high-frequency waves propagating in the generated anisotropic models are computed using the generalized Dix formula (Grechka et al., 1999). Figure 3 shows that the effective NMO ellipses $\mathbf{W}^e$ in our 300 vastly different anisotropic models overlap (thin solid

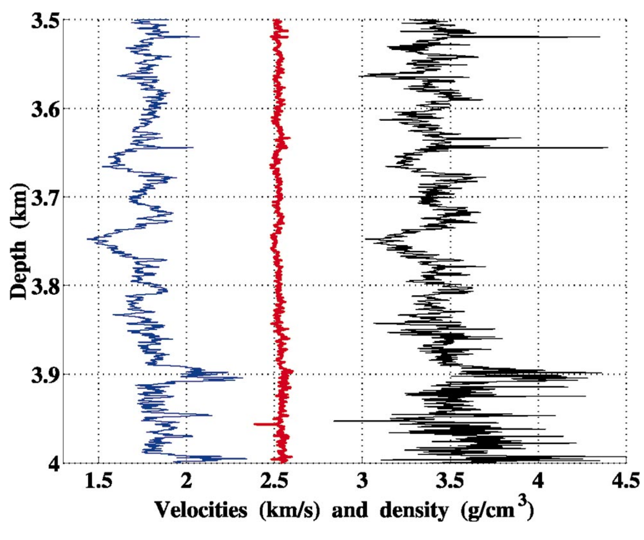

FIG. 1. Sonic (black), shear (blue), and density (red) logs. We treat sonic and shear logs as the vertical velocities V_{P0} and V_{S0}, respectively.

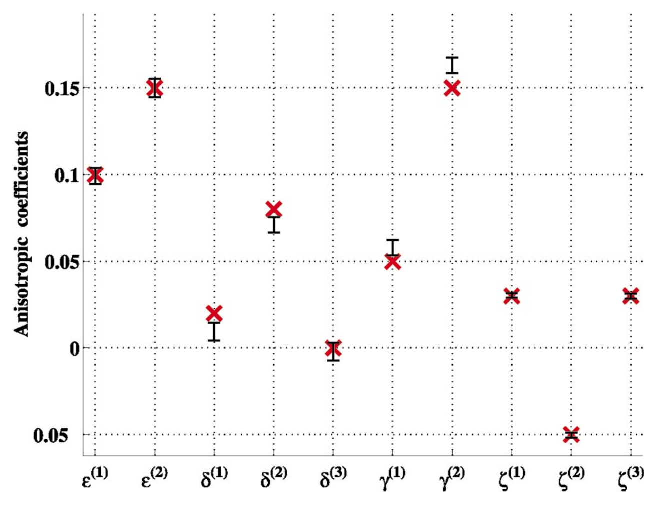

FIG. 2. Mean values of interval anisotropic coefficients (crosses) and ranges of their effective values Δ^e (bars) obtained for 300 models.

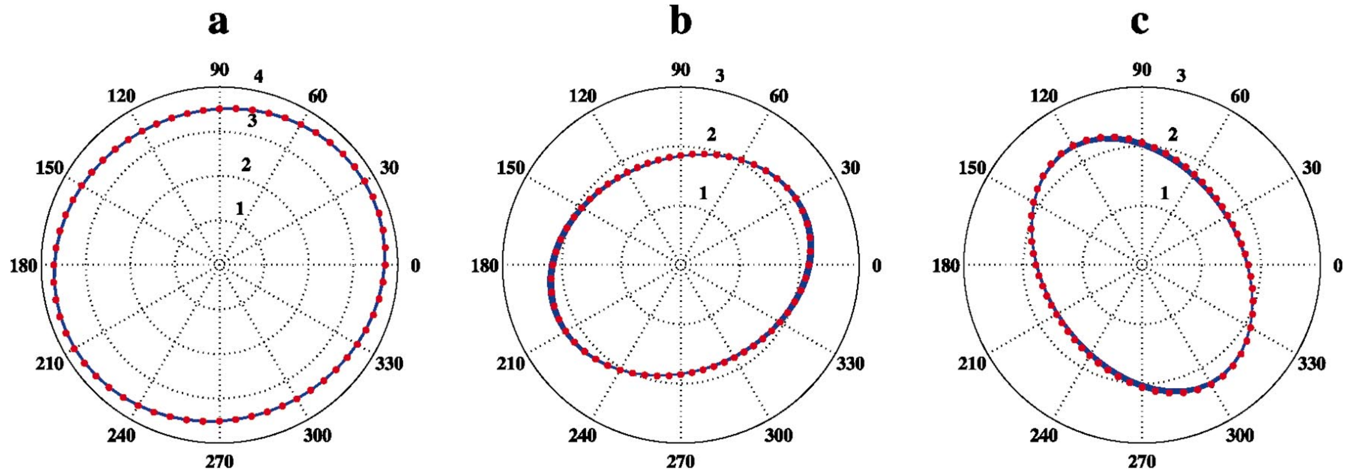

FIG. 3. NMO ellipses $\bar{\mathbf{W}}$ of (a) P-, (b) S_1-, and (c) S_2-waves computed in the mean model (red dots) and ellipses $\mathbf{W}^e$ obtained by applying generalized Dix formula in 300 models with randomly varying anisotropy (solid). The circles marked with 1, 2, 3, 4 indicate velocities (in km/s); the numbers 0, 30, ..., 330 correspond to azimuths (in degrees) in the horizontal plane.

lines). More importantly, the ellipses $\bar{\mathbf{W}}$ computed in the mean model (red dots in Figure 3) match the exact ones. Although this could have been predicted from the correspondence of the mean and effective anisotropic coefficients shown in Figure 2, the performed test demonstrates that robustness of formula (16) does not seem to depend on frequency content of the data.

DISCUSSION AND EXTENSIONS

The main result of our paper is given by the equality $\mathbf{m}^e = \bar{\mathbf{m}} + O(\tilde{\mathbf{m}}^2)$. It not only shows that the effective parameters can be approximately replaced with the mean values of interval ones (this has been noticed before for particular models), but it also indicates the high accuracy of this substitution when fluctuations of local parameters are relatively small. We demonstrated the validity of this statement for a typical well log that was intentionally made anisotropic. While it is clear that the accuracy of approximation $\mathbf{m}^e \approx \bar{\mathbf{m}}$ deteriorates as the parameter fluctuations increase, the presented test as well as others (not shown) indicate that heterogeneity should be rather strong to render our results useless.

It is interesting that the equation $\mathbf{m}^e = \bar{\mathbf{m}} + O(\tilde{\mathbf{m}}^2)$ is formally valid for any effective quantity and for any frequency of propagating waves. We illustrated this by comparing the mean anisotropy $\bar{\mathbf{\Delta}}$ with the effective ones given by Schoenberg-Muir and generalized Dix averages which, strictly speaking, correspond to zero and infinite frequencies. A similar result for velocities and attenuation in layered isotropic structures was obtained by Shapiro and Hubral (1996). They explicitly showed that frequency-dependent phase increments and attenuation coefficients do not contain the linear terms in velocity and density fluctuations [their equations (5) and (6)]. The absence of linear terms in either Shapiro and Hubral's or our equations indicates that replacing $\bar{\mathbf{m}}$ with harmonic or geometric or any other average will not significantly alter the predicted effective quantities. In fact, Beretta et al. (2001) noticed this for the P- and S-wave transit times in 1D finely layered media. All averaging techniques they tested led to the times that differed from each other by less than 2%.

Finally, the generality of derivation presented here also suggests that our main result remains valid not only for 1D but also for 3D anisotropic heterogeneous media (Appendix A). Indeed, since the above introduced averaging operation $\mathbf{F}$ is rather arbitrary, there is no apparent reason to restrict our final conclusion to just horizontally layered solids. While we are not aware of any exact solutions that could be used to verify the last statement for general anisotropy and heterogeneity, certain approximations indicate that such extensions are natural. For instance, Gold et al. (2000) and Müller et al. (2002) showed that both the effective velocity and so-called effective scattering attenuation contain only quadratic and higher-order terms in $\tilde{\mathbf{m}}$ in 2D and 3D random media. As their result is consistent with our prediction that differences between the volume-averaged and effective quantities are proportional to the squared local fluctuations, it can be taken as an independent verification of the theory described in this paper.

ACKNOWLEDGMENTS

We thank Shell International E&P Inc. for permission to publish the paper and the reviewers for useful suggestions.

REFERENCES

Backus, G. E., 1962, Long-wave elastic anisotropy produced by horizontal layering: J. Geophys. Res., **67**, 4427–4440.
Bakulin, A., 2003, Intrinsic and layer-induced vertical transverse isotropy: Geophysics, **68**, 1708–1713.
Beretta, M. M., Bernasconi, G., Colombo, A., and Drufuca, G., 2001, Comparison of averaging processes for equivalent fine layered media: 63rd Conf. Eur. Assn. Geosci. Eng., Extended Abstracts, P-095.
Christensen, R. M., 1979, Mechanics of composite materials: Wiley, New York.
Dix, C. H., 1955, Seismic velocities from surface measurements: Geophysics, **20**, 68–86.
Gold, N., Shapiro, S. A., Bojinski, S., and Müller, T. M., 2000, An approach to upscaling for seismic waves in statistically isotropic heterogeneous elastic media: Geophysics, **65**, 1837–1850.
Grechka, V., Contreras, P., and Tsvankin, I., 2000, Inversion of normal moveout for monoclinic media: Geophysical Prospecting, **48**, 577–602.
Grechka, V., and Tsvankin, I., 2002, Processing-induced anisotropy: Geophysics, **67**, 1920–1928.
Grechka, V., Tsvankin, I., and Cohen, J. K., 1999, Generalized Dix equation and analytic treatment of normal-moveout velocity for anisotropic media: Geophysical Prospecting, **47**, 117–148.

Müller, T. M., Shapiro, S. A., and Sick, C. M. A., 2002, Most probable ballistic waves in random media: A weak-fluctuation approximation and numerical results: Waves in Random Media, **12**, 223–245.
Schoenberg, M., and Muir, F., 1989, A calculus for finely layered anisotropic media: Geophysics, **54**, 581–589.
Shapiro, S. A., and Hubral, P., 1996, Elastic waves in finely layered sediments: The equivalent medium and generalized O'Doherty-Anstey formulas: Geophysics, **61**, 1282–1300.
Thomsen, L., 1986, Weak elastic anisotropy: Geophysics, **51**, 1954–1966.

APPENDIX A

EFFECTIVE STIFFNESS COEFFICIENTS FOR 3D HETEROGENEOUS ANISOTROPIC MEDIA

To illustrate the generality of equation (3), we show that it describes the effective stiffness coefficients in 3D heterogeneous anisotropic media. To this end, we define the function **F** as

$$\mathbf{F}[\mathbf{c}(\mathbf{x})] \equiv \mathbf{c}(\mathbf{x})\varepsilon(\mathbf{x}), \qquad \text{(A-1)}$$

where **c** is the stiffness tensor, ε is the strain tensor, and **x** denotes cartesian coordinates. Since equation (A-1) represents Hooke's law, we can write

$$\mathbf{F}[\mathbf{c}(\mathbf{x})] \equiv \mathbf{c}(\mathbf{x})\varepsilon(\mathbf{x}) = \boldsymbol{\tau}(\mathbf{x}), \qquad \text{(A-2)}$$

where $\boldsymbol{\tau}$ is the stress tensor. Similar definition for the effective stiffnesses, strains, and stresses reads

$$\mathbf{F}[\mathbf{c}^e] \equiv \mathbf{c}^e\varepsilon^e = \boldsymbol{\tau}^e. \qquad \text{(A-3)}$$

The relationship between the effective and local stress tensors (e.g., Christensen, 1979),

$$\boldsymbol{\tau}^e = \frac{1}{V}\int_V \boldsymbol{\tau}(\mathbf{x})d\mathbf{x}, \qquad \text{(A-4)}$$

allows us to construct the following sequence of equalities:

$$\mathbf{F}[\mathbf{c}^e] = \boldsymbol{\tau}^e = \frac{1}{V}\int_V \boldsymbol{\tau}(\mathbf{x})d\mathbf{x} = \frac{1}{V}\int_V \mathbf{c}(\mathbf{x})\varepsilon(\mathbf{x})d\mathbf{x} = \frac{1}{V}\int_V \mathbf{F}[\mathbf{c}(\mathbf{x})]d\mathbf{x}. \qquad \text{(A-5)}$$

As follows from the fist and last equations in our sequence and the second equation (2),

$$\mathbf{c}^e = \mathbf{F}^\dagger\left[\frac{1}{V}\int_V \mathbf{F}[\mathbf{c}(\mathbf{x})]d\mathbf{x}\right], \qquad \text{(A-6)}$$

which is exactly equation (3) in the main text. The function $\mathbf{F}^\dagger$ here denotes solving linear equations (A-3) with respect to $\mathbf{c}^e$.